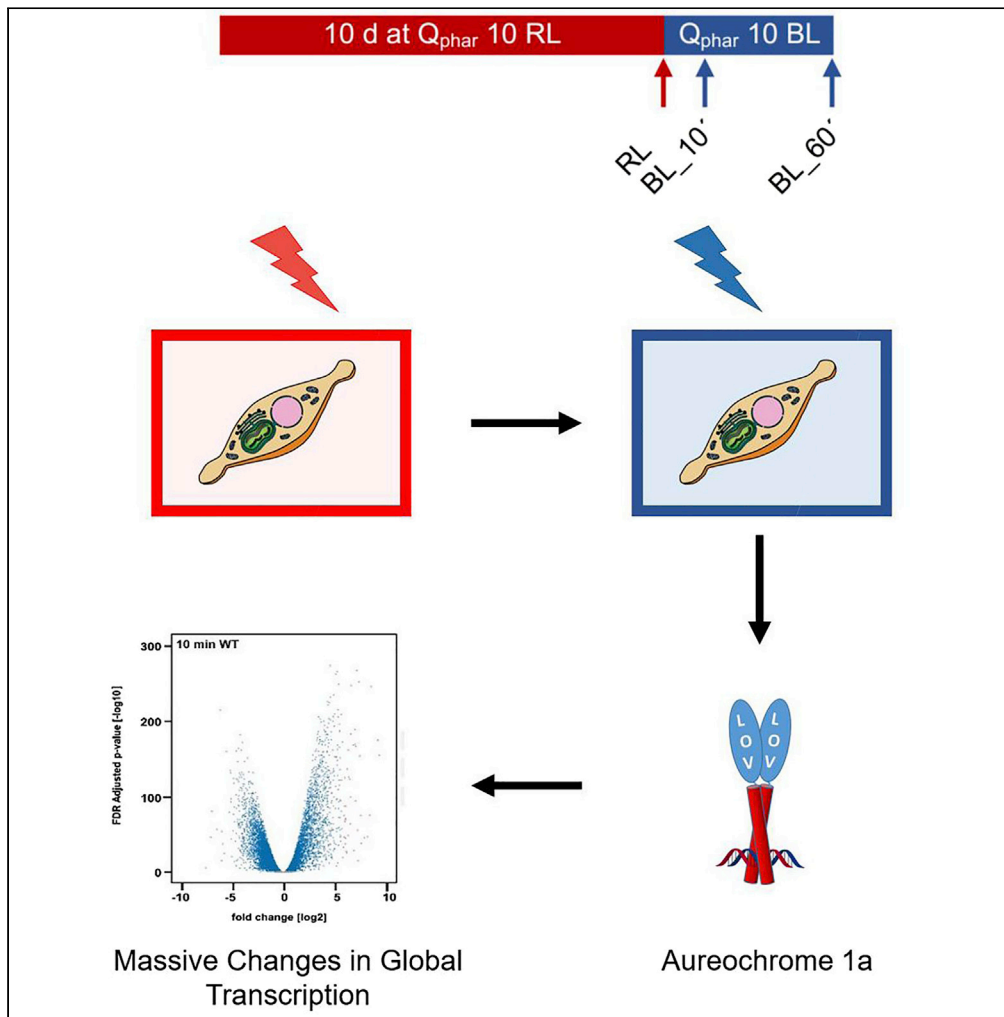


Article

The Aureochrome Photoreceptor PtAUREO1a Is a Highly Effective Blue Light Switch in Diatoms



Marcus Mann,
Manuel Serif,
Thomas
Wrobel, ...,
Bernard Lepetit,
Christian Wilhelm,
Peter G. Kroth

peter.kroth@uni-konstanz.de

HIGHLIGHTS

Blue light induces a very fast transcriptional response in the diatom *P. tricornutum*

This strong response is almost completely inhibited when Aureochrome 1a is absent

The results imply a key role of PtAureo 1a in blue light-induced responses in diatoms



Article

The Aureochrome Photoreceptor PtAUREO1a Is a Highly Effective Blue Light Switch in Diatoms

Marcus Mann,^{1,5} Manuel Serif,^{2,4,5} Thomas Wrobel,^{3,5} Marion Eisenhut,³ Shvaita Madhuri,² Samantha Flachbart,³ Andreas P.M. Weber,³ Bernard Lepetit,² Christian Wilhelm,¹ and Peter G. Kroth^{2,6,*}

SUMMARY

Aureochromes represent a unique type of blue light photoreceptors that possess a blue light sensing flavin-binding LOV-domain and a DNA-binding bZIP domain, thus being light-driven transcription factors. The diatom *Phaeodactylum tricorutum*, a member of the essential marine primary producers, possesses four aureochromes (PtAUREO1a, 1b, 1c, 2). Here we show a dramatic change in the global gene expression pattern of *P. tricorutum* wild-type cells after a shift from red to blue light. About 75% of the genes show significantly changed transcript levels already after 10 and 60 min of blue light exposure, which includes genes of major transcription factors as well as other photoreceptors. Very surprisingly, this light-induced regulation of gene expression is almost completely inhibited in independent PtAureo1a knockout lines. Such a massive and fast transcriptional change depending on one single photoreceptor is so far unprecedented. We conclude that PtAUREO1a plays a key role in diatoms upon blue light exposure.

INTRODUCTION

Diatoms are unicellular photoautotrophic algae that gained their plastids from secondary endosymbiosis (Archibald, 2015), in which a heterotrophic eukaryote engulfed a primitive unicellular red alga and converted it into a plastid (Cavalier-Smith, 2013). During this process, the resulting chimeric organism temporarily possessed five different genomes, two within the eukaryotic nuclei of host and endosymbiont, and three prokaryotic genomes within the mitochondria of the host and endosymbiont cell as well as one in the chloroplast. The nucleus and the mitochondria of the endosymbiont meanwhile have vanished in diatoms. Hence, a preceding massive gene transfer from the nucleus of the endosymbiont to the nucleus of the secondary host cell has to be assumed, leading to newly recombined genes and gene functions (Gruber, 2019; Nonoyama et al., 2019). Recent genome sequencing analyses showed that the diatom nuclear genome contains genes related to those of both plants and animals, including the green algal lineage, as well as a rather high percentage of bacterial genes due to lateral gene transfer (Bowler et al., 2008; Mock et al., 2017; Moustafa et al., 2009). In addition to their complex genome organization, diatoms differ in many aspects from green algae: Their cell walls consist of silica, the chloroplasts have a peculiar ultrastructure with four surrounding membranes, and the thylakoids are arranged in bands of three (Tanaka et al., 2015). Also, the basic pathways for energy conversion and carbon partitioning show a number of unusual features compared with higher plants and green or red algae (Bailleul et al., 2015; Flori et al., 2017). These genetic and physiological characteristics of diatoms are in line with an extremely fast evolution (Sims et al., 2006), leading to an estimated 100,000 diatom species (Adl et al., 2012). These evolutionary peculiarities coincide with an extraordinary ecological success: diatoms exist in nearly all aquatic and humid environments, encompassing oceans and freshwaters including their sediments, as well as soils, and aerophytic biofilms (Armbrust, 2009; Malviya et al., 2016). The diversity and environmental adaptability might be explained by the increased genetic background that may allow enhanced and unknown environmental acclimation strategies against a broad spectrum of stressors, e.g., light intensity (Lepetit et al., 2013; Wilhelm et al., 2014), UV-B (Beardall et al., 2009), as well as carbon dioxide and iron limitation (Goldman et al., 2019; Kolody et al., 2019).

For a photosynthetic organism, it is essential to determine and respond to changes in light quality and quantity. As land plants do, diatoms can sense light intensity via the activity of their photosystems and

¹Institut für Biologie, Universität Leipzig, 04009 Leipzig, Germany

²Fachbereich Biologie, Universität Konstanz, 78457 Konstanz, Germany

³Institut für Biochemie der Pflanzen, Cluster of Excellence on Plant Science (CEPLAS), Heinrich-Heine-Universität, 40225 Düsseldorf, Germany

⁴Present address: Department of Biology, Norwegian University of Science and Technology, 7491 Trondheim, Norway

⁵These authors contributed equally

⁶Lead Contact

*Correspondence: peter.kroth@uni-konstanz.de
<https://doi.org/10.1016/j.isci.2020.101730>



additionally possess photoreceptors that allow the sensing of both light intensity as well as wavelengths, including the diatom phytochromes (DPH) (Fortunato et al., 2016), different cryptochromes (cry) (König et al., 2017), heliorhodopsins (Pushkarev et al., 2018), and aureochromes (Kroth et al., 2017; Mativ and Chekunova, 2018). Aureochromes have first been described in the siphonous xanthophyte *Vaucheria frigida* (Takahashi et al., 2007). They are very peculiar, as they are found in stramenopile algae only (Suetsugu and Wada, 2013), and they contain both a Flavin-binding LOV domain for blue light absorption and a bZIP domain for DNA binding (Takahashi et al., 2007). Thus, aureochromes essentially are light-responsive transcription factors and their simple topology makes them natural candidates for optogenetic tools in transcriptional regulation (Hepp et al., 2020). The common domain topology is inverted compared with all other characterized LOV proteins, with the sensory domain being located at the C terminus of the LOV receptor (Herman and Kottke, 2015). bZIP domains have a general tendency to dimerize, and only the dimeric bZIP domain is capable of binding DNA. For some aureochromes, dimerization and DNA binding have been shown to be induced by blue light (Banerjee et al., 2016b; Hisatomi et al., 2014; Nakatani and Hisatomi, 2015). However, the oligomerization state of full-length aureochromes is under debate. In the dark, PtAUREO1a has been observed as a monomer in equilibrium with a dimer (Heintz and Schlichting, 2016) or as a dimer/higher oligomer (Banerjee et al., 2016b). Light induces the dimerization of LOV domains and the association of the monomers (Herman et al., 2013; Goett-Zink et al., 2020; Kobayashi et al., 2020), which is the rate-limiting step in the process of DNA binding (Akiyama et al., 2016). The diatom *P. tricornutum* contains four genes encoding different aureochromes (Schellenberger Costa et al., 2013). Although all of them possess a LOV domain, only three of the respective gene products (PtAUREO1a/b/c) can actually bind a flavin, constituting the functional chromophore that allows detection of blue light (Banerjee et al., 2016b; Schellenberger Costa et al., 2013). The fourth aureochrome, PtAUREO2, carries a conserved mutation preventing flavin binding (Banerjee et al., 2016b), similarly to AUREO2 orthologs from other organisms.

Interestingly, the expression of some aureochromes follows a different diurnal pattern (Banerjee et al., 2016b), and there is evidence for a function of PtAUREO1a in cell cycle regulation (Huysman et al., 2013). Although previously created PtAureo1a silencing lines indicate an involvement of PtAUREO1a in triggering photosynthetic acclimation to different light colors and intensities (Schellenberger Costa et al., 2013), the influence of PtAUREO1a on the diatom transcriptome is yet unknown. It was the aim of this study to analyze the changes in the cellular transcriptome profile of the wild-type (WT) cells, PtAUREO1a-deficient mutants, as well as complemented lines of *P. tricornutum* after full acclimatization to red light and a subsequent shift to blue light. Importantly, for the light shift, we changed the wavelength, but not the number of photons absorbed by the photosystems, in order to exclude potential retrograde signaling effects induced by plastidic redox changes (Lepetit et al., 2013). Because it is known that in gene-silenced cell lines the amount of the investigated protein may be variable, we here chose to compare WT cells with two independent PtAureo1a knockout lines (Serif et al., 2017).

Our results demonstrate a dramatic change in the transcriptome upon shifting cells from red to blue light, affecting most cellular processes. This response is massively reduced in the PtAureo1a knockout lines, indicating a key role of the PtAUREO1a protein in cellular acclimation to blue light. As proteins that are known to be central in blue light responses in Archaeplastida, e.g., COP1 or HY5 (Podolec and Ulm, 2018), apparently are missing in diatoms, a fundamentally different regulation of blue light responses has to be assumed in diatoms and related algae.

RESULTS

Dramatic Changes in *P. tricornutum* WT Cells When Shifted from Red to Blue Light

In order to elucidate the impact of the transcription factor PtAUREO1a on the global expression pattern of *P. tricornutum* cells, we decided to monitor expression changes after a maximal change of the light trigger from red to blue light. We acclimated *P. tricornutum* WT cells (strain Pt4) for 10 days to red light, followed by a direct shift to blue light. As monochromatic red and blue light are differentially absorbed by the photosynthetic pigments in the diatom plastids, the light intensities were adjusted to an identical amount of photosynthetically absorbed light radiation (Q_{phar}, calculated according to Gilbert et al., 2000) of 10 μmol photons m⁻² s⁻¹. We sampled in biological triplicates and generated transcriptomes that refer to the state directly before the shift as well as 10 and 60 min after the change of the light condition (Figure 1A) in order to observe the dynamics of this process. We had decided for the relatively short times of 10 and 60 min, because we expected that aureochromes as transcription factors may induce changes

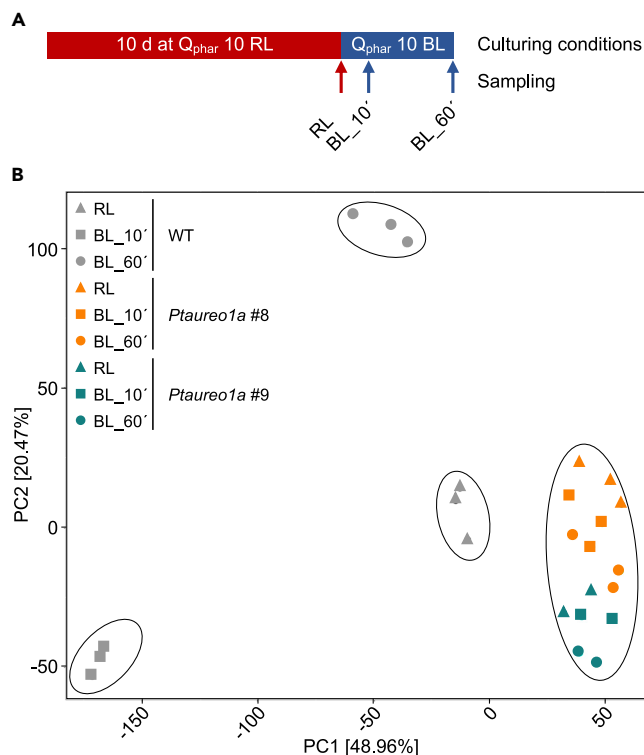


Figure 1. Transcriptomic Analyses of *P. tricornutum* Cells after a Shift from Red Light to Blue Light

WT cells (three biological replicates), two independent *Ptaureo1a* mutant cells lines, *Ptaureo1a* #8 (three biological replicates) and #9 (two biological replicates), were studied.

(A) Scheme depicting the cultivation of the cell lines for 10 days at red light, followed by a shift to blue light comprising the identical amount of photosynthetically absorbed light quanta (Q_{phar}). Samples were taken directly before the light shift (RL), and 10 (BL 10') and 60 min (BL 60') after the light shift.

(B) Principal component analysis (PCA) shows initial changes for component 1 and long-term changes for component 2. WT samples in the same acclimation state, as well as all *Ptaureo1a* mutant samples, are encircled.

in gene transcription rapidly. Mapping of RNA-seq reads to the *P. tricornutum* genome (Phatr3, protists.ensembl.org/Phaeodactylum_tricornutum) identified 10,854 differentially expressed genes (87.6% of total genes). For the quantitative analyses reported here, only statistically significant changes of transcript abundance with a Benjamini-Hochberg corrected q-value of <0.01 were taken into account (Benjamini and Hochberg, 1995). In the WT, the principal component analysis (PCA) shows a dramatic change of total gene expression after the shift from red to blue light (Figure 1B). The three independent replicates of each time point consistently group together, whereas the samples of the individual time points show a clear separation (Figure 1B). The initial shift is covered in principal component 1 that explains 48.96% of the total variation, whereas the long-term reaction is mainly associated with principal component 2 that explains 20.47% of the total variation. This indicates that drastic changes in the gene expression pattern already occur 10 min after the shift to blue light, which differs strongly from the pattern at 60 min. Plotting probability values against \log_2 -fold changes (Figure S1) indicates that the total number of upregulated genes is higher after 10 min, whereas the number of downregulated genes becomes higher after 60 min (both compared with the 0 min sample). After 10 min, about 74% of the genes are differentially regulated. About 60 min after the light shift, the number of non-regulated genes increased slightly to 39%, whereas about 30% of genes each are either up- or downregulated.

In a hierarchical cluster analysis, we could identify eight clusters with different expression patterns (Figure 2A, gray lines): In clusters 1–5, gene expression decreases after 10 min, whereas clusters 6–8 show an increase of gene expression after 10 min. However, only in clusters 1, 2, and 6 the increase/decrease is sustained after 60 min, whereas the other clusters return back to the original expression at $t = 0$ in a more or less strongly pronounced way or show the opposite response. Interestingly, clusters 4 and 5 show a strong decrease after 10 min, whereas, after 60 min, the expression values are higher than the

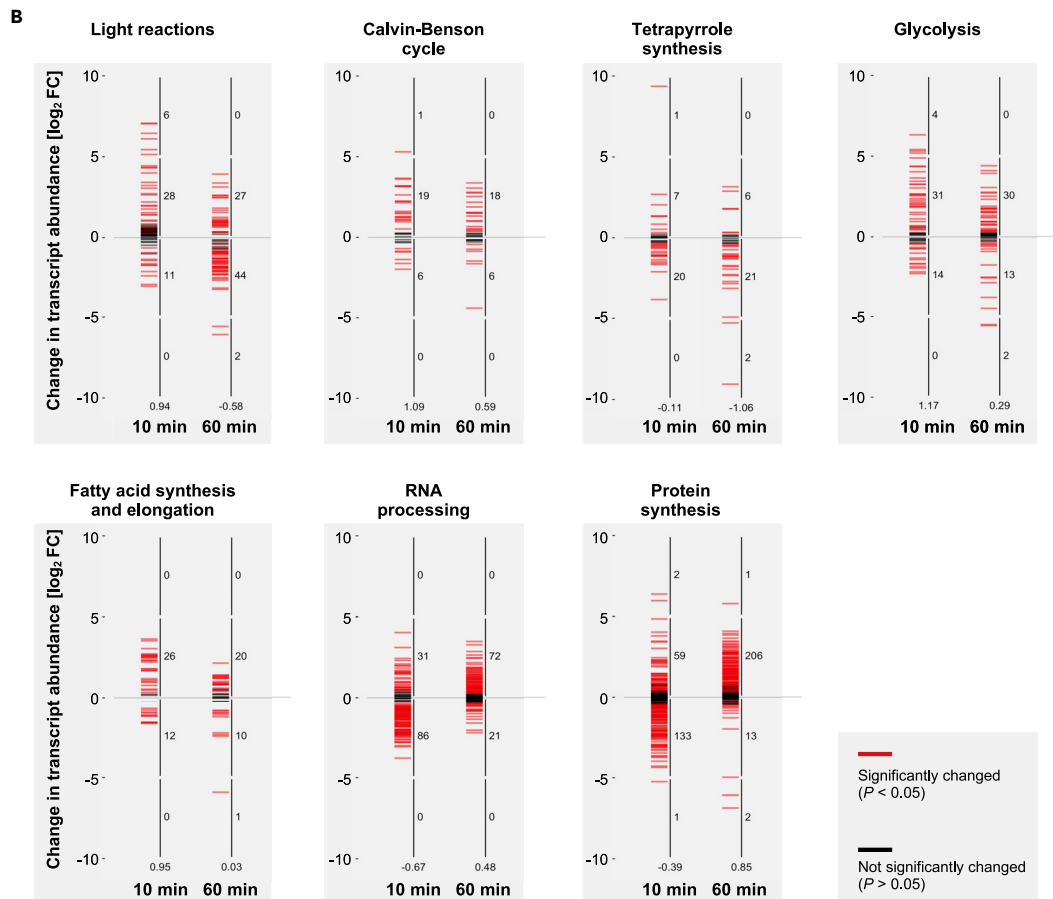
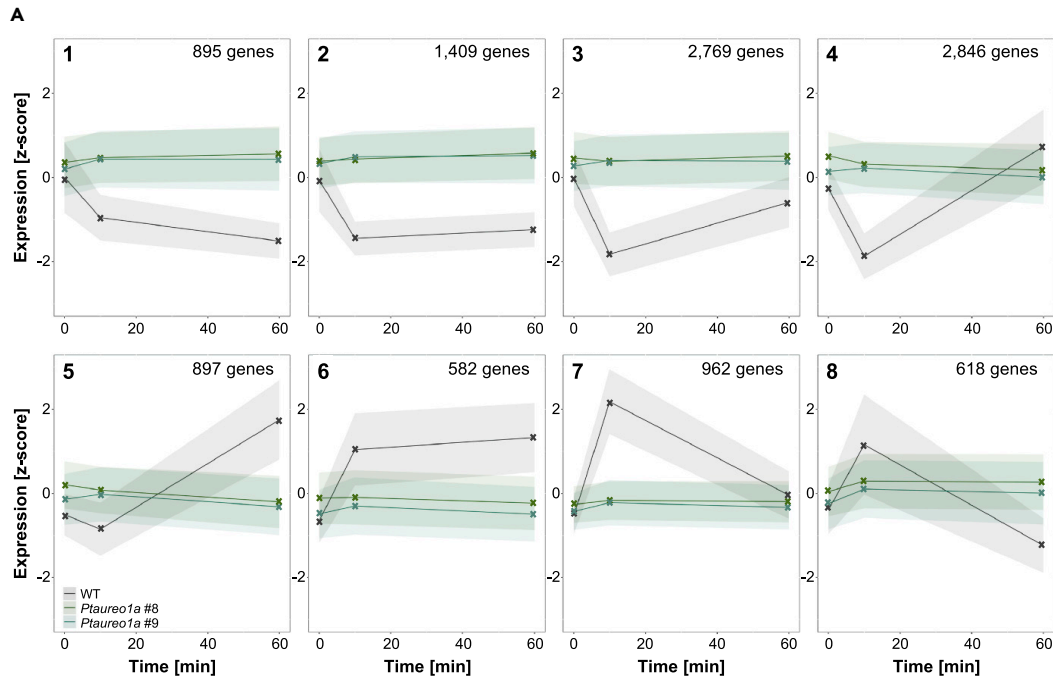


Figure 2. Clustering of Transcripts According to Blue Light Responses of Genes of Selected Pathways

(A) We identified eight clusters that show different responses 10 and 60 min after a shift to blue light. The gray area indicates the range of transcript numbers of the WT cells, the green areas that of the two mutant cell lines. Where the area of both mutant lines overlaps, it is depicted in a darker green.

(B) Clustering of up- and downregulated genes in WT cells in specific pathways that show a clear tendency. The y axis refers to \log_2 -fold change at the respective time point compared with time point 0 (FC = fold change). The small numbers at the right side of the vertical axis indicate the number of genes regulated in the respective \log_2 -fold interval covering five units, and the small number below the y axis refers to the average \log_2 -fold change of all genes of this pathway.

starting point. The opposite behavior can be observed in cluster 8. When sorting genes according to gene ontology (GO), it becomes obvious that specifically the number of genes encoding enzymes of the light reaction, the Calvin-Benson cycle, glycolysis, and fatty acid metabolism, are strongly upregulated, especially after 10 min of blue light exposure. Instead, the majority of genes involved in tetrapyrrole synthesis is down-regulated (Figure 2B). Pathways that are involved in generation of proteins, e.g., genes encoding enzymes involved in RNA elongation and protein synthesis, interestingly show a strong down-regulation after 10 min, followed by an upregulation after 60 min.

In order to investigate how a shift to blue light may lead to such a quick response, we studied the expression of transcription factors more closely. A total of 214 transcription factors have been identified so far in the genome of *P. tricornutum* (Rayko et al., 2010; Matthijs et al., 2017), of which 210 could be detected and identified within our transcriptome dataset. Illumination with blue light results in a fast and pronounced response among these transcription factors: exposure to blue light for 10 min yielded a significant transcript increase of 40% and decrease of 42% of transcription factors, whereas after 60 min blue light exposure, 29% of transcription factor genes were upregulated and 33% were downregulated (Table 1). When the two different blue light samples (10 and 60 min) were compared with each other, it became apparent that these were in different adaptive states, with 33% of transcription factors upregulated and 44% downregulated after 60 min in comparison with the shorter blue light exposure. Thus, a short-term and a longer-term regulation can be seen in the WT cells, similarly to what was observed for the whole transcriptome. In order to identify groups of transcription factors that are more influenced by blue light exposure than others, we here examined the most prominent classes of transcription factors known in *P. tricornutum* in more detail. A total of 70 HSFs (heat shock factors), 40 zinc finger proteins, 34 Myb factors, 23 bZIP (basic leucine zipper domain) transcription factors, and 7 bHLH proteins together correspond to 81% of all transcription factors found in *P. tricornutum* (Rayko et al., 2010; Matthijs et al., 2017) (Table 1). In the WT cells, the shift from red to blue light led to a significant up- or downregulation of most of the members of these transcription factor classes after 10 min (see also Figure S2). The prolonged blue light treatment of 60 min resulted in more than 50% of transcripts of all major transcription factor classes to be up- or downregulated compared with the red light conditions. The large family of HSFs were substantially affected here with over 51% of transcripts downregulated and 17% upregulated at BL₆₀, respectively, whereas about 50% of the bZIP factors show an increased transcript abundance after 10 min.

Differential Gene Expression in PtAureo1a Knockout Mutants

Previous studies revealed a regulatory function of PtAUREO1a in different processes such as high light acclimation and cell cycle (Huysman et al., 2013; Schellenberger Costa et al., 2013). In order to unravel the general function in blue light responses, we examined PtAureo1a knockout mutants in an identical experimental setting as described for the WT cells, including the same growth conditions and acclimation to red light. The knockout strains *Ptaureo1a#8* and *Ptaureo1a#9* had been created previously by genome editing via TALENs (Serif et al., 2017), and they have been characterized in detail to ensure that the PtAureo1a expression is abolished completely in both mutant lines (Serif et al., 2017). Moreover, the phenotypes of the mutants have been verified previously by complementation studies (Madhuri et al., 2019) to verify that in these mutants only the PtAureo1a gene had been affected. We observed that both PtAUREO1a-deficient strains, in contrast to the WT cells, show a very similar but weaker response to blue light. Figure 1B reveals that (1) the data points of *Ptaureo1a#8* (in biological triplicate samples) and *Ptaureo1a#9* (in duplicate samples) are located very close to each other, (2) the data points of the mutants all cluster close to the WT samples at time point 0, and (3) the samples of the individual mutants cluster closely together, irrespective of whether they were taken at time point 0, 10, or 60 min. This clearly indicates that the PtAureo1a knockout mutants respond very weakly to blue light, thus behaving very differently compared with the WT cells. This also becomes obvious when examining the response clusters (Figure 2A, green lines). In all clusters, the WT cells respond in one or the other way described above, whereas the mutant cell lines hardly respond at all.

Transcription Factors	Regulation	WT_10 min_BL	WT_60 min_BL	WT_60 min/10 min_BL
All (214)	Up	86 (40%)	62 (29%)	71 (33%)
	Down	89 (42%)	70 (33%)	96 (44%)
HSF (70)	Up	26 (37%)	12 (17%)	18 (26%)
	Down	34 (49%)	36 (51%)	32 (71%)
Myb (34)	Up	9 (26%)	11 (32%)	17 (50%)
	Down	17 (50%)	7 (21%)	10 (29%)
bZIP (23)	Up	12 (52%)	4 (17%)	3 (13%)
	Down	6 (26%)	11 (48%)	17 (74%)
Zinc finger (40)	Up	17 (43%)	13 (33%)	17 (43%)
	Down	16 (40%)	9 (23%)	14 (35%)
bHLH (7)	Up	3 (43%)	3 (43%)	1 (14%)
	Down	2 (29%)	1 (14%)	5 (71%)

Table 1. Effect of Blue Light Treatment on Transcript Levels of Transcription Factors

Given are numbers of significantly up-/down-regulated genes belonging to five important transcription factor classes found in *P. tricornutum* together with percentages with regard to all factors of that group (in parentheses). The total number of members of each group is given in parentheses (HSF, heat shock factors; Myb; bZIP, basic region leucine zipper; Zinc finger; bHLH, basic-helix-loop-helix).

We found that the two independent PtAureo1a knockout lines investigated here had very similar transcription profiles that are clearly distinct from those of the WT cells. We verified this result independently by qPCR-based gene expression analyses of two independent PtAureo1a complemented lines (Madhuri et al., 2019). We here focused on four genes, which exhibited a strong differential expression between WT and PtAureo1a knockout lines (UDP glucose pyrophosphorylase, HSF2, glycerol-3-phosphate dehydrogenase, and the gene Phatr3_J38559, see Figure S3). Although the culture conditions were not completely identical for technical reasons, the results confirm that the massive changes in gene expression upon a red to blue light shift, which are strongly dampened in the two PtAureo1a knockout lines, is re-established in the two PtAureo1a complemented lines to a similar extent as in the WT.

As we monitored the transcriptome during changes in light color, we specifically investigated gene expression regulation of PtAureo1a, 1b, 1c, 2 (Figure 3) and that of other diatom photoreceptors (Figure 4). Looking at the transcript abundances of PtAureo1a in the WT cells, we found that they are already comparably high at RL, whereas they are strongly reduced 10 min after the shift to blue light and close to zero after 60 min (Figure 3A). Similarly to PtAureo1a, the PtAureo1b and PtAureo2 genes in WT cells are downregulated after blue light induction, whereas in the PtAureo1a knockout mutants, the transcript abundances of PtAureo1b and PtAureo2 are not affected by blue light, remaining on the previous red light level (Figures 3B and 3D). PtAureo1c shows the opposite response: transcription is induced by blue light, whereas in the mutant lines transcription remains unregulated on a very low level (Figure 3C). We also examined the response of transcript abundances of the other photoreceptors in *P. tricornutum*. Diatoms possess a number of cryptochrome-like proteins, for which it is not exactly known whether they primarily function in DNA repair or in blue light signaling (König et al., 2017). The cryptochrome/photolyase family proteins PtCPF1 and 2 are strongly upregulated by blue light in WT cells, while more weakly responding in the PtAureo1a KO mutants (Figures 4A and 4B). PtCPF4 transcripts are reduced after 10 min blue light in WT cells, while not responding in both PtAureo1a knockout mutants. The three cyclobutane pyrimidine dimer photolyases PtCPD1,3,4 show a different response (Figures 4D–4F): PtCPD1 is upregulated by blue light in WT cells, whereas the transcription of PtCPD3 is repressed and PtCPD4 instead is unaffected. All three genes, though, show a different mRNA pattern in the mutant lines, which is closer to the time point 0 in WT cells. The cryptochrome PtCryP shows a slight increase 10 min after the switch to blue light, whereas after 60 min, essentially no transcripts are detectable (Figure 4G). The red light-absorbing diatom phytochrome PtDPH1 shows inhibition of transcription by blue light in WT cells and no change in the knockout lines (Figure 4H). Finally, also the recently discovered heliorhodopsin PtHeR shows an impact of blue light on transcripts in

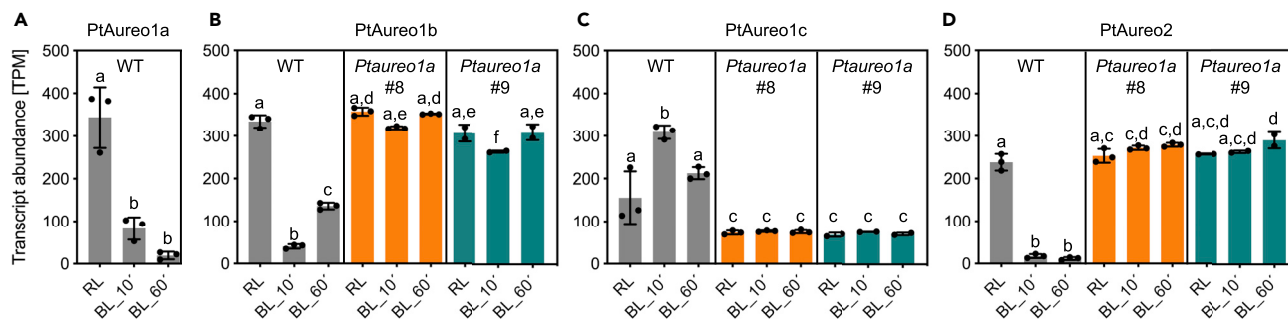


Figure 3. Transcript Abundance in TPM (Transcript per Million) of the Four Aureochrome Genes PtAureo1a/1b/1c/2

WT cells and two independent PtAureo1a knockout lines (PtAureo1a #8 and #9) were studied (A: PtAureo1a; B: PtAureo1b; C: PtAureo1c; D: PtAureo2). For each gene, the average transcript abundance is shown for samples at time points 0, 10, 60 min after the light shift from red (RL) to blue (BL) light. Identical y axes have been chosen to allow a comparison of the transcript abundances. Statistics were performed using two-way ANOVA with Tukey test to correct for multiple comparisons. TPM values were called significantly different if the adjusted p value ≤ 0.05 . Letters indicate statistical significance. TPM values sharing letters are not significantly different.

the WT cells but not in the PtAureo1a knockout mutants (Figure 4I). Taken together, transcript amounts of all of these light-absorbing signaling proteins clearly show different dynamics in WT and in mutant lines, indicating that PtAUREO1a may modulate, directly or indirectly, their expression. Interestingly, most of the photoreceptors exhibited a comparable transcript level at time point 0 (thus in red light) in WT and KO mutants except for PtAureo1c (Figure 3C), which was lower in the mutants even at time point zero.

As we had observed a massive regulation of transcription factors upon a red to blue light shift in the WT, we also compared the regulation of selected transcription factors in the PtAureo1a KO lines (Figure 5). We found very dramatic changes for PtbZIP10/11/18/21b, which all are strongly induced after 10 min blue light in the WT cells but which do not change much in the PtAureo1a mutants at the different time points. PtAUREO1a has previously been shown to be involved in both photoprotection and cell cycle progression after dark arrest (Huysman et al., 2013; Schellenberger Costa et al., 2013; Serif et al., 2017), the latter in cooperation with bZIP10 (Huysman et al., 2013). Interestingly, transcription of bZIP10 in WT is strongly upregulated upon blue light treatment for 10 min but downregulated after 60 min (and not induced in the mutant lines). Conversely, PtbZIP15 and the transcription factor PtPSR show a decreased transcript abundance after 10 min and a very strong increase after 60 min, which is not observed in the mutant lines. PtZIP14 instead shows a generally higher transcript abundance in the mutant lines. Overall, the studied bZIP transcription factors like PtbZIP10 and PtbZIP18 revealed a rather high transcript abundance. PtbHLH1a (RITMO1), which recently has been shown to be involved in the circadian regulation of *P. tricornutum* (Annunziata et al., 2019), is strongly transcribed after 10 min, and to a lesser extent after 60 min, which is mirrored much weaker in the mutant lines. Interestingly, PtbHLH1b, which is related to RITMO1, shows a very similar but even more pronounced expression pattern.

Finally, we also examined genes that are involved in post-translational modifications (PTMs) of histones like acetyl-transferases, deacetylases, and methyl-transferases (Figure S4). Interestingly, most of the genes encoding PTM-related proteins were less expressed in WT cells compared with PtAureo1a KO mutants at all time points. However, the most pronounced changes in transcription of PTM genes between WT cells and PtAureo1a KO were observed after 10 min, indicating that PtAureo1a is required for regulating the histone PTMs.

DISCUSSION

Photoreceptors are important for cellular acclimation, a dynamic process that includes sensing of environmental signals, and signaling to the nucleus in order to change gene expression, and cellular/organismic remodeling eventually. Light acclimation has been studied intensively in diatoms, showing that a shift from low to high light induces a reduction in light harvesting antenna size, and an increase of components of electron transport and C-assimilation, but also leads to higher activities of photoprotection, N-assimilation, protein biosynthesis, carbohydrate storage, nutrient transporters, and cell proliferation (Smith et al., 2019; Wilhelm et al., 2014). In green algae, the mechanism triggering this cellular

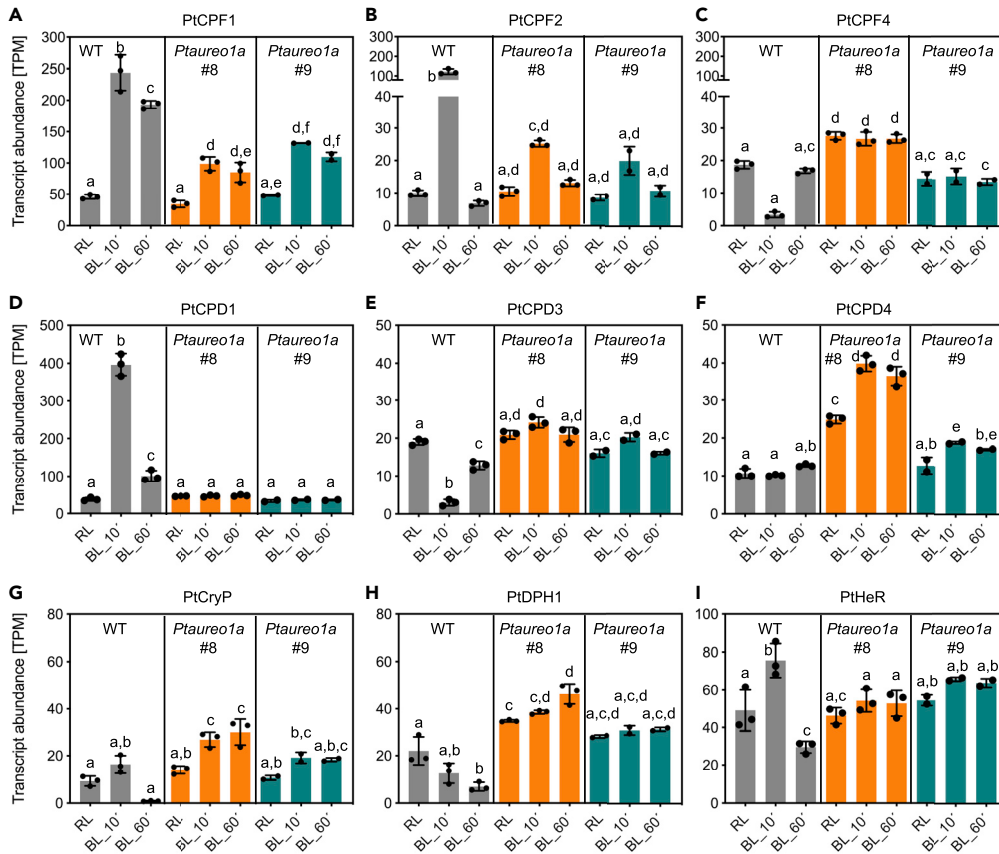


Figure 4. Transcript Abundance in TPM (Transcript per Million) of Genes of Diatom Photoreceptors and Related Proteins

Transcript abundance of (A) PtCPF1, (B) PtCPF2, (C) PtCPF4 (cryptochrome photolyase family), (D) PtCPD1, (E) PtCPD3, (F) PtCPD4 (cyclobutane pyrimidine dimer photolyases), (G) the plant like cryptochrome PtCryP, (H) the diatom phytochrome PtDHP1, (I) the heliorhodopsin PtHeR in wild-type cells and in two independent *PtAureo1a* knockout lines (*PtAureo1a* #8 and #9) are shown. For each gene, the average transcript abundance is shown for samples at time points 0, 10, 60 min after the light shift from red (RL) to blue (BL) light. Note that here different y axes have been chosen because of the large TPM differences. Statistics were performed using two-way ANOVA with Tukey test to correct for multiple comparisons. TPM values were called significantly different if the adjusted p value ≤ 0.05 . Letters indicate statistical significance. TPM values sharing letters are not significantly different.

reorganization is closely linked to the light-dependent redox state of the cells (reviewed in Burlacot et al., 2019). In diatoms, the redox state of the PQ pool is also involved in light acclimation reactions (Lepetit et al., 2013), but the redox control machinery in the plastid via the redox regulator thioredoxin is different from that of green algae (Matsuda and Kroth, 2014). Recently, it was shown that the light acclimation ability in diatoms instead is strongly dependent on the aureochrome photoreceptor system (Schellenberger Costa et al., 2013), which is lacking in the green lineage. PtbHLH1a (also called RITMO1) is involved in regulation of circadian rhythm of diatoms (Annunziata et al., 2019). Transcription of RITMO1 in our experiment is increased by about 30-fold upon blue light exposure for 10 min, suggesting that its rhythmicity might be triggered by activation of aureochromes and/or other photoreceptors. Especially for benthic diatoms, it has been shown that minor changes in their location within the sediments can already have a strong impact on wavelength-specific light attenuation (Cartaxana et al., 2016), requiring adequate responses. Aureochromes can affect gene expression directly, and such a direct interaction with promoters may result in faster responses to light changes compared with other photoreceptors that are relying on signal cascades that include, e.g., phosphorylation steps (Duanmu et al., 2017). We observed that blue light strongly influenced gene expression of genes of the Calvin cycle, the photosynthetic light reaction, the tetrapyrrole biosynthesis, and the lipid metabolism (Figure 2B). These processes are directly affected by available light intensity and color, as they may buffer a potential excess of light

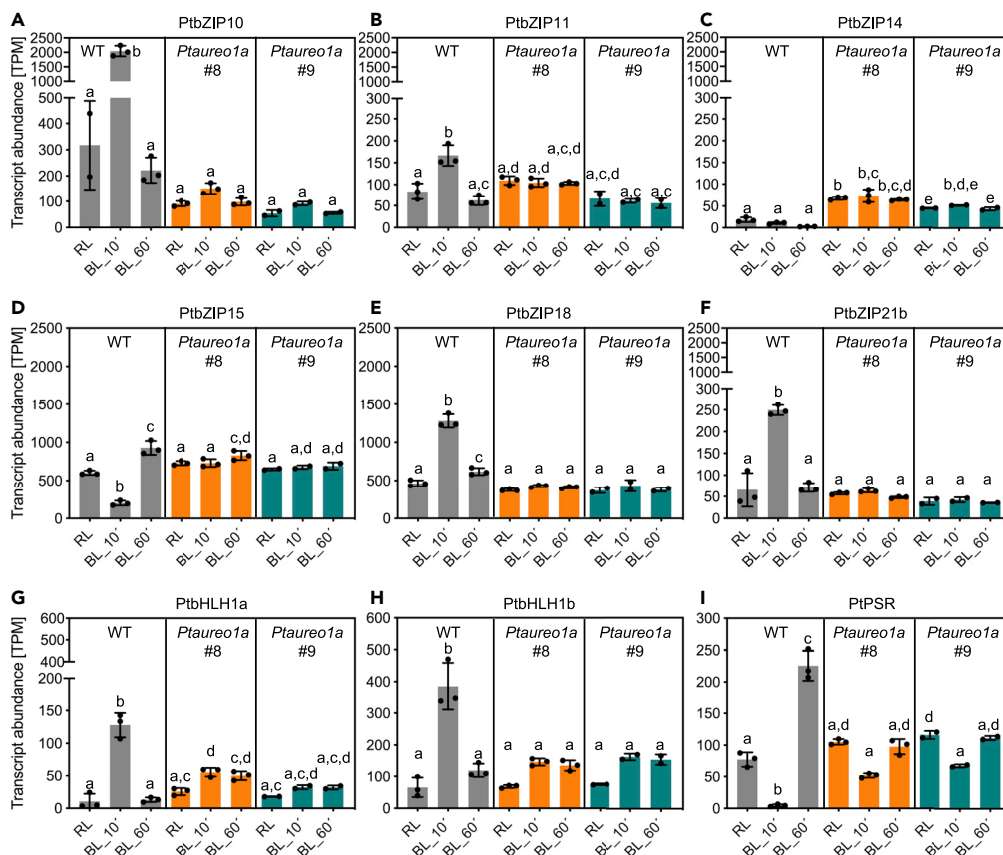


Figure 5. Transcript Abundance in TPM (Transcript per Million) of Genes of Selected Transcription Factors

Transcript abundance of (A) PtbZIP10, (B) PtbZIP11, (C) PtbZIP14, (D) PtbZIP15, (E) PtbZIP18, (F) PtbZIP21b, the basic-helix-loop-helix transcription factors (G) PtbHLH1a (RITMO1) and (H) PthHL1b, and (I) the Myb1R_SHAQKYF5 transcription factor (PtPSR) in wild-type cells and two independent PtAureo1a knockout lines (*PtAureo1a #8* and *#9*) are shown. For each gene, the average transcript abundance is shown for samples at time points 0, 10, 60 min after the light shift from red (RL) to blue (BL) light. Identical y axes have been chosen for two groups to allow a comparison of the transcript abundances. Statistics were performed using two-way ANOVA with Tukey test to correct for multiple comparisons. TPM values were called significantly different if adjusted p value ≤ 0.05 . Letters indicate statistical significance. TPM values sharing letters are not significantly different.

energy, for which blue light can be indicative. Indeed, in the PtAureo1a knockout mutants these responses are much weaker (see Table S3).

One important observation of this and previous work is that knocking out PtAUREO1a is not lethal but results in specific phenotypes like a reduced light acclimation and a drastically reduced blue light response. This indicates that the aureochromes in *P. tricornutum* may have specific functions, and, at least in case of PtAUREO1a, cannot complement each other. Instead, they may form a self-controlling network, similarly to land plant phytochromes and the respective PIF transcription factors (Legris et al., 2019). The expression and function of aureochromes in *P. tricornutum* can be regulated on different levels: First, the transcription of the aureochromes shows different diel patterns: the expression of PtAureo1a and 1c follows a diel cycle, whereas transcription of the PtAureo1b gene is light induced (Banerjee et al., 2016b). Second, we here observed that, in addition to this circadian control, PtAureo1b, 1c, and 2 show a different expression pattern in the PtAureo1a KO mutant lines: PtAureo1a, under blue light, has a negative impact on the expression of the PtAureo1b and 2 genes, whereas PtAureo1c transcription requires the presence and stimulation of PtAUREO1a (Figure 3). We further could show that all PtAureo genes are highly expressed under red light conditions in WT cells, whereas transcription of PtAureo1a, 1b, and 2 is strongly downregulated after 10 and 60 min of blue light exposure. This indicates that aureochromes themselves and—as the PtAureo genes are regulated in WT but not in PtAureo1a KO lines—apparently no other blue light receptor

may inhibit the expression of these aureochromes or that red light is required for their transcription. PtAureo1c is the only aureochrome that shows an increased transcription after a change to blue light in WT cells. A third mode of aureochrome regulation is the potential formation of heterodimers with other aureochromes or possibly other bZIP transcription factors (Banerjee et al., 2016b). This makes a discussion on the exact regulatory role of PtAUREO1a more complicated, as we do not know yet, whether (1) the absence of PtAUREO1a homodimers in the mutant lines is responsible for the drastic decrease of blue light induction, or whether (2) other aureochromes or bZIP factors may require PtAUREO1a as partner for heterodimer formation. Indeed, hetero-dimerization of PtAUREO1a and PtAUREO1c has been demonstrated *in vitro* (Banerjee et al., 2016a; Essen et al., 2017).

Although some of the previous investigations on externally induced changes in gene expression in *P. tricornutum* focused on long-term acclimation (Cruz de Carvalho et al., 2016; Huang et al., 2019), others also took short-term changes into consideration. Bones and coworkers showed that *P. tricornutum* responds strongly to light exposure after 48 h in complete darkness, and also to equal doses of red, green, and blue light (Nymark et al., 2013; Valle et al., 2014). Although these experiments were performed via microarrays that cover only a number of pre-selected genes, thus giving limited insights into global gene expression, they demonstrate the strongest responses 30 min after the light shift, which is the earliest time point investigated in that work (Nymark et al., 2013). This clearly supports our hypothesis that the fast changes that we observed are most likely based on photoreceptors and a quick conversion of the response via transcription factors. Smith et al. (2019) studied the response of *P. tricornutum* to a shift from nitrogen to ammonium and found about 50% of all genes responding to N-deplete or N-replete conditions; binning of the responding genes resulted in 201 distinct clusters or response types. Although cluster selection can be done in different ways and to different extent, this number is much larger than the numbers of cluster that we obtained for the blue light response. This may indicate that nutrient responses are much less hierarchically initiated and conveyed than the responses to blue light that are transmitted via PtAureo1a.

So far, we have a very fragmented knowledge about aureochrome-mediated signaling processes. In land plants, photoreceptors lack DNA-binding motifs and therefore do not interact directly with promoters. Instead, complex light-induced developmental processes require interaction of the photoreceptors with key regulators like COP1/SPA and HY5, which either interact with other proteins or serve as transcription factors, multiplying the responses and controlling processes like photomorphogenesis (Hoecker, 2017; Podolec and Ulm, 2018). As such systems so far have not been identified in diatoms and other stramenopiles, these algae likely developed a different regulatory system that relies on aureochromes that are both photoreceptors and transcription factors. Genetic regulation in plants like *A. thaliana* depends much more on transcription factors than it may be the case in diatoms, which may reflect their higher morphological complexity. Although approximately 5% of the total genes in *A. thaliana* are estimated to be transcription factors (Riechmann et al., 2000), in *P. tricornutum* transcription factor genes only represent about 2% of its total genes (Rayko et al., 2010). Nonetheless, the 214 identified transcription factors (Rayko et al., 2010) in *P. tricornutum* allow an astonishingly and unprecedented strong response within a very short time frame of 10 min, majorly initiated by PtAUREO1a.

Given the huge number of affected genes including the drastic changes in transcript pattern of transcription factors, it seems though unlikely that the huge impact on cellular transcription, which is observed in the WT cells, but absent in the PtAureo1a knockout lines, is based on individual interaction of PtAUREO1a with all respective promoters. This notion is supported by our finding that PtAureo1a expression at time point 0 is not particularly high, compared with that of the other transcription factors (based on TPM values). It seems more likely that, besides a putative direct interaction of PtAUREO1a homodimers and heterodimers with promoters of target genes (see above), PtAUREO1a may be involved in changes of the expression of other transcription factors, which themselves are responsible for gene regulation (including that of other transcription factor genes). Such a cascade of transcription factor activities could explain the wide response by the limited number of PtAUREO photoreceptors, representing an equivalent to the signal cascades of other photoreceptors that are based on phosphorylation/dephosphorylation of signaling components, modulating gene transcription via more than one step. This described regulation may also occur in red light conditions, as we observed that transcripts of several transcription factors are virtually absent in PtAureo1a KO lines in red light, and therefore should not be able to influence gene expression already after 10 min of BL.

Besides the activity of transcription factors, the enzymatic modification of histones, for instance, by deacetylases and methylases, may have a strong impact on transcriptional activity. Such post-translational (PTM)

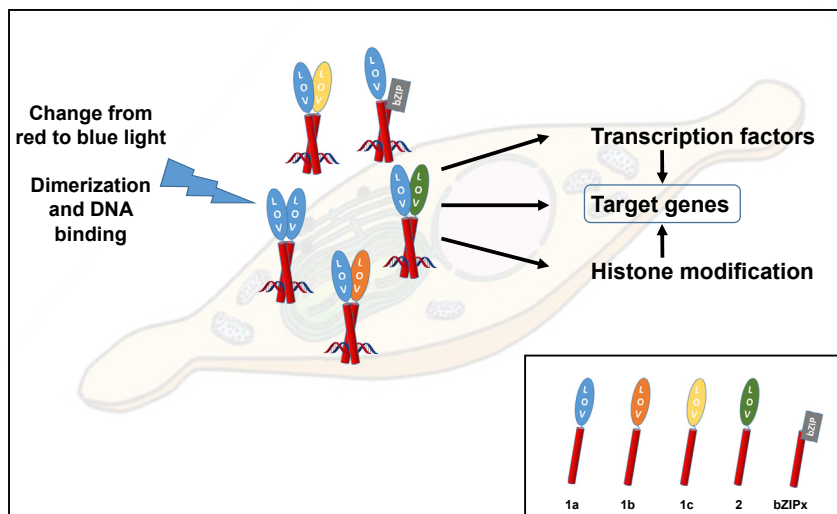


Figure 6. Hypothetical Model Describing the Impact of Aureochrome 1a (AUREO1a) on Gene Expression in *P. tricornutum*

In the right lower corner, the individual aureochrome monomers and an exemplary bZIP protein are shown. PtAUREO1a, upon activation by blue light, may form homodimers, heterodimers with other aureochromes, or heterodimers with other bZIP proteins and bind to promoters. PtAUREO dimers may affect genes directly, and also via the transcriptional regulation of transcription factors, as well as by regulating the expression of histone modifying enzymes.

activity has also been described recently for *P. tricornutum* (Veluchamy et al., 2013). As we could show that most of the genes known to be involved in PTMs are expressed to a lower degree in WT cells compared with PtAureo1a KO mutant lines, especially after the shift to blue light for 10 min (Figure S4), we hypothesize that histone modification may play an important role in PtAUREO1a-mediated responses (Figure 6).

In conclusion, it was very surprising to see that the deletion of a single blue light receptor (PtAUREO1a) has such a strong impact on gene expression, even though the cells possess several blue light receptors. This indicates that PtAUREO1a plays a central role in the perception of blue light by the algae. It may act on different regulatory levels, which include (1) the direct regulation of genes either as homo-dimers, aureochrome heterodimers, or heterodimers with other bZIP proteins like PtbZIP10 (Huysman et al., 2013), (2) the direct or indirect control of different transcription factors, and (3) the regulation of histone modifications. The aureochrome system of diatoms may serve as a future model to elucidate both top-down signaling cascades triggered by a single protein as well as diatom-specific regulatory mechanisms.

Limitations of the Study

Here we show that diatom transcription responds dramatically to blue light and that mostly aureochrome 1a is responsible for this response. Aureochromes are only found in Stramenopile algae, which include different algal groups, like the ecologically important diatoms, chrysophytes, and brown algae. The results thus cannot be used directly to understand better the light regulation in land plants. We also have to proof experimentally in future analyses, which other transcription factors in which order are specifically involved in transmitting aureochrome-induced responses to such a large number of promoters.

Resource Availability

Lead Contact

Further information and requests for resources should be directed to and will be fulfilled by the Lead Contact, Peter Kroth (peter.kroth@uni-konstanz.de).

Materials Availability

The strain used in this study (*P. tricornutum* Pt4, UTEX#646) is available from the UTEX Culture Collection (<https://utex.org>).

Data and Code Availability

The read data are deposited at the National Center for Biotechnology Information Gene Expression Omnibus (GEO) under accession number GSE158698. The datasets generated and analyzed during this study are available in the [Supplemental Information](#).

METHODS

All methods can be found in the accompanying [Transparent Methods supplemental file](#).

SUPPLEMENTAL INFORMATION

Supplemental Information can be found online at <https://doi.org/10.1016/j.isci.2020.101730>.

ACKNOWLEDGMENTS

P.G.K., M.S., M.M., C.W. have been supported by the German Research Foundation (Deutsche Forschungsgemeinschaft, DFG) within the program FOR1261 (projects KR1661/8-1/2, WI 764/19-1/2) and by project KR1661/19-1. B.L. acknowledges funding by the DFG (project LE 3358/3-1/2). P.G.K. is also thankful to the Gordon and Betty Moore Foundation for support (project GBMF 4966 “DiaEdit”). T.W., M.E., A.P.M.W. appreciate funding by the DFG under Germany’s Excellence Strategy – EXC-2048/1 –project ID 390686111.

AUTHOR CONTRIBUTIONS

Conceptualization: P.G.K., C.W., M.E., A.P.M.W.; Methodology: M.M., M.S., T.W., M.E., S.M., S.F., B.L., C.W., P.G.K.; Formal analysis: M.M., M.S., T.W., M.E., B.L., C.W., P.G.K.; Investigation: M.M., M.S., T.W.; Writing – Original Draft: P.G.K., C.W., B.L.; Writing – Review and Editing: P.G.K., C.W., B.L., M.E., M.S., A.P.M.W.; Funding Acquisition: P.G.K., C.W., A.P.M.W.; Supervision: P.G.K., C.W., B.L., M.E.

DECLARATION OF INTERESTS

The authors declare no competing interests.

Received: July 29, 2020

Revised: September 30, 2020

Accepted: October 21, 2020

Published: November 20, 2020

REFERENCES

- Adl, S.M., Simpson, A.G.B., Lane, C.E., Lukeš, J., Bass, D., Bowser, S.S., Brown, M.W., Burki, F., Dunthorn, M., Hampel, V., et al. (2012). The revised classification of eukaryotes. *J. Eukaryot. Microbiol.* 59, 429–514.
- Akiyama, Y., Nakasone, Y., Nakatani, Y., Hisatomi, O., and Terazima, M. (2016). Time-resolved detection of light-induced dimerization of monomeric aureochrome-1 and change in affinity for DNA. *J. Phys. Chem. B* 120, 7360–7370.
- Annunziata, R., Ritter, A., Fortunato, A.E., Manzotti, A., Cheminant-Navarro, S., Agier, N., Huysman, M.J.J., Winge, P., Bones, A.M., Bouget, F.-Y., et al. (2019). bHLH-PAS protein RITMO1 regulates diel biological rhythms in the marine diatom *Phaeodactylum tricornutum*. *Proc. Natl. Acad. Sci. U S A*, 13137–13142.
- Archibald, John M. (2015). Endosymbiosis and eukaryotic cell evolution. *Curr. Biol.* 25, R911–R921.
- Armbrust, E.V. (2009). The life of diatoms in the world’s oceans. *Nature* 459, 185–192.
- Bailleul, B., Berne, N., Murik, O., Petroustos, D., Prihoda, J., Tanaka, A., Villanova, V., Bligny, R., Flori, S., Falconet, D., et al. (2015). Energetic coupling between plastids and mitochondria drives CO₂ assimilation in diatoms. *Nature* 524, 366–369.
- Banerjee, A., Herman, E., Kottke, T., and Essen, L.-O. (2016a). Structure of a native-like aureochrome 1a LOV domain dimer from *Phaeodactylum tricornutum*. *Structure* 24, 171–178.
- Banerjee, A., Herman, E., Serif, M., Maestre-Reyna, M., Hepp, S., Pokorny, R., Kroth, P.G., Essen, L.-O., and Kottke, T. (2016b). Allosteric communication between DNA-binding and light-responsive domains of diatom class I aureochromes. *Nucleic Acids Res.* 44, 5957–5970.
- Beardall, J., Sobrino, C., and Stojkovic, S. (2009). Interactions between the impacts of ultraviolet radiation, elevated CO₂, and nutrient limitation on marine primary producers. *Photochem. Photobiol. Sci.* 8, 1257–1265.
- Benjamini, Y., and Hochberg, Y. (1995). Controlling the false discovery rate: a practical and powerful approach to multiple testing. *J. R. Stat. Soc. Ser. B (Methodological)* 57, 289–300.
- Bowler, C., Allen, A.E., Badger, J.H., Grimwood, J., Jabbari, K., Kuo, A., Maheswari, U., Martens, C., Maumus, F., Otilar, R.P., et al. (2008). The *Phaeodactylum* genome reveals the evolutionary history of diatom genomes. *Nature* 456, 239–244.
- Burlacot, A., Peltier, G., and Li-Beisson, Y. (2019). Subcellular energetics and carbon storage in *chlamydomonas*. *Cells* 8, 1154.
- Cartaxana, P., Ribeiro, L., Goessling, J.W., Cruz, S., and Kühl, M. (2016). Light and O₂ microenvironments in two contrasting diatom-dominated coastal sediments. *Mar. Ecol. Prog. Ser.* 545, 35–47.
- Cavalier-Smith, T. (2013). Symbiogenesis: mechanisms, evolutionary consequences, and systematic implications. *Annu. Rev. Ecol. Evol. Syst.* 44, 145–172.
- Cruz de Carvalho, M.H., Sun, H.-X., Bowler, C., and Chua, N.-H. (2016). Noncoding and coding transcriptome responses of a marine diatom to

- phosphate fluctuations. *New Phytol.* 210, 497–510.
- Duanmu, D., Rockwell, N.C., and Clark Lagarias, J. (2017). Algal light sensing and photoacclimation in aquatic environments. *Plant Cell Environ.* 40, 2558–2570.
- Essen, L.-O., Franz, S., and Banerjee, A. (2017). Structural and evolutionary aspects of algal blue light receptors of the cryptochrome and aureochrome type. *J. Plant Physiol.* 217, 27–37.
- Flori, S., Jouneau, P.-H., Bailleul, B., Gallet, B., Estrozi, L.F., Moriscot, C., Bastien, O., Eicke, S., Schober, A., Bártulos, C.R., et al. (2017). Plastid thylakoid architecture optimizes photosynthesis in diatoms. *Nat. Commun.* 8, 15885.
- Fortunato, A.E., Jaubert, M., Enomoto, G., Bouly, J.-P., Raniello, R., Thaler, M., Malviya, S., Bernardes, J.S., Rappaport, F., Gentili, B., et al. (2016). Diatom phytochromes reveal the existence of far-red light based sensing in the ocean. *Plant Cell* 28, 616–628.
- Gilbert, M., Domin, A., Becker, A., and Wilhelm, C. (2000). Estimation of primary productivity by chlorophyll *a* in vivo fluorescence in freshwater phytoplankton. *Photosynthetica* 38, 111–126.
- Goett-Zink, L., Klocke, J.L., Bögeholz, L.A.K., and Kottke, T. (2020). In-cell infrared difference spectroscopy of LOV photoreceptors reveals structural responses to light altered in living cells. *J. Biol. Chem.* 295, 11729–11741.
- Goldman, J.A.L., Schatz, M.J., Berthiaume, C.T., Coesel, S.N., Orellana, M.V., and Armbrust, E.V. (2019). Fe limitation decreases transcriptional regulation over the diel cycle in the model diatom *Thalassiosira pseudonana*. *PLoS One* 14, e0222325.
- Gruber, A. (2019). What's in a name? How organelles of endosymbiotic origin can be distinguished from endosymbionts. *Microb. Cell (Graz, Austria)* 6, 123–133.
- Heintz, U., and Schlichting, I. (2016). Blue light-induced LOV domain dimerization enhances the affinity of Aureochrome 1a for its target DNA sequence. *Elife* 5, e11860.
- Herman, E., Sachse, M., Kroth, P.G., and Kottke, T. (2013). Blue-light-induced unfolding of the J α helix allows for the dimerization of aureochrome-LOV from the diatom *Phaeodactylum tricornutum*. *Biochemistry* 52, 3094–3101.
- Herman, E., and Kottke, T. (2015). Allosterically regulated unfolding of the A' α helix exposes the dimerization site of the blue-light-sensing aureochrome-LOV domain. *Biochemistry* 54, 1484–1492.
- Hepp, S., Trauth, J., Hasenjäger, S., Bezold, F., Essen, L.O., and Taxis, C. (2020). An optogenetic tool for induced protein stabilization based on the *Phaeodactylum tricornutum* aureochrome 1a light-Oxygen-Voltage domain. *J. Mol. Biol.* 432, 1880–1900.
- Hisatomi, O., Nakatani, Y., Takeuchi, K., Takahashi, F., and Kataoka, H. (2014). Blue light-induced dimerization of monomeric aureochrome-1 enhances its affinity for the target sequence. *J. Biol. Chem.* 289, 17379–17391.
- Hoecker, U. (2017). The activities of the E3 ubiquitin ligase COP1/SPA, a key repressor in light signaling. *Curr. Opin. Plant Biol.* 37, 63–69.
- Huang, R., Ding, J., Gao, K., Cruz de Carvalho, M.H., Tirichine, L., Bowler, C., and Lin, X. (2019). A Potential role for epigenetic processes in the acclimation response to elevated pCO₂ in the model diatom *Phaeodactylum tricornutum*. *Front. Microbiol.* 9, 3342.
- Huysman, M.J., Fortunato, A.E., Matthijs, M., Costa, B.S., Vanderhaeghen, R., Van den Daele, H., Sachse, M., Inze, D., Bowler, C., Kroth, P.G., et al. (2013). AUREOCHROME1a-mediated induction of the diatom-specific cyclin dsCYC2 controls the onset of cell division in diatoms (*Phaeodactylum tricornutum*). *Plant Cell* 25, 215–228.
- Kobayashi, I., Nakajima, H., and Hisatomi, O. (2020). Molecular mechanism of light-induced conformational switching of the LOV domain in aureochrome-1. *Biochemistry* 59, 2592–2601.
- Kolody, B.C., McCrow, J.P., Allen, L.Z., Aylward, F.O., Fontanez, K.M., Moustafa, A., Moniruzzaman, M., Chavez, F.P., Scholin, C.A., Allen, E.E., et al. (2019). Diel transcriptional response of a California current plankton microbiome to light, low iron, and enduring viral infection. *ISME J.* 2817–2833.
- König, S., Juhas, M., Jäger, S., Kottke, T., and Büchel, C. (2017). The cryptochrome—photolyase protein family in diatoms. *J. Plant Physiol.* 217, 15–19.
- Kroth, P.G., Wilhelm, C., and Kottke, T. (2017). An update on aureochromes: phylogeny – mechanism – function. *J. Plant Physiol.* 217, 20–26.
- Legris, M., Ince, Y.C., and Fankhauser, C. (2019). Molecular mechanisms underlying phytochrome-controlled morphogenesis in plants. *Nat. Commun.* 10, 5219.
- Lepetit, B., Sturm, S., Rogato, A., Gruber, A., Sachse, M., Falcitore, A., Kroth, P.G., and Lavaud, J. (2013). High light acclimation in the secondary plastids containing diatom *Phaeodactylum tricornutum* is triggered by the redox state of the plastoquinone pool. *Plant Physiol.* 161, 853–865.
- Madhuri, S., Rio Bártulos, C., Serif, M., Lepetit, B., and Kroth, P.G. (2019). A strategy to complement PtAUREO1a in TALEN knockout strains of *Phaeodactylum tricornutum*. *Algal Res.* 39, 101469.
- Malviya, S., Scalco, E., Audic, S., Vincent, F., Veluchamy, A., Poulain, J., Wincker, P., Iudicone, D., de Vargas, C., Bittner, L., et al. (2016). Insights into global diatom distribution and diversity in the world's ocean. *Proc. Natl. Acad. Sci. U S A* 113, E1516–E1525.
- Matiiv, A.B., and Chekunova, E.M. (2018). Aureochromes - blue light receptors. *Biochemistry (Mosc.)* 83, 662–673.
- Matsuda, Y., and Kroth, P. (2014). Carbon fixation in diatoms. In *The Structural Basis of Biological Energy Generation*, M.F. Hohmann-Marriott, ed. (Springer Netherlands), pp. 335–362.
- Matthijs, M., Fabris, M., Obata, T., Foubert, I., Franco-Zorrilla, J.M., Solano, R., Fernie, A.R., Vyverman, W., and Goossens, A. (2017). The transcription factor bZIP14 regulates the TCA cycle in the diatom *Phaeodactylum tricornutum*. *EMBO J.* 36, 1559–1576.
- Mock, T., Otilar, R.P., Strauss, J., McMullan, M., Paajanen, P., Schmutz, J., Salamov, A., Sanges, R., Toseland, A., Ward, B.J., et al. (2017). Evolutionary genomics of the cold-adapted diatom *Fragilariopsis cylindrus*. *Nature* 541, 536–540.
- Moustafa, A., Beszteri, B., Maier, U.G., Bowler, C., Valentin, K., and Bhattacharya, D. (2009). Genomic footprints of a cryptic plastid endosymbiosis in diatoms. *Science* 324, 1724–1726.
- Nakatani, Y., and Hisatomi, O. (2015). Molecular mechanism of photozipper, a light-regulated dimerizing module consisting of the bZIP and LOV domains of aureochrome-1. *Biochemistry* 54, 3302–3313.
- Nonoyama, T., Kazamia, E., Nawaly, H., Gao, X., Tsuji, Y., Matsuda, Y., Bowler, C., Tanaka, T., and Dorrell, R.G. (2019). Metabolic innovations underpinning the origin and diversification of the diatom chloroplast. *Biomolecules* 9, 322.
- Nymark, M., Valle, K.C., Hancke, K., Winge, P., Andresen, K., Johnsen, G., Bones, A.M., and Brembu, T. (2013). Molecular and photosynthetic responses to prolonged darkness and subsequent acclimation to re-illumination in the diatom *Phaeodactylum tricornutum*. *PLoS One* 8, e58722.
- Podolec, R., and Ulm, R. (2018). Photoreceptor-mediated regulation of the COP1/SPA E3 ubiquitin ligase. *Curr. Opin. Plant Biol.* 45, 18–25.
- Pushkarev, A., Inoue, K., Larom, S., Flores-Uribe, J., Singh, M., Konno, M., Tomida, S., Ito, S., Nakamura, R., Tsunoda, S.P., et al. (2018). A distinct abundant group of microbial rhodopsins discovered using functional metagenomics. *Nature* 558, 595–599.
- Rayko, E., Maumus, F., Maheswari, U., Jabbari, K., and Bowler, C. (2010). Transcription factor families inferred from genome sequences of photosynthetic stramenopiles. *New Phytol.* 188, 52–66.
- Riechmann, J.L., Heard, J., Martin, G., Reuber, L., Jiang, C.-Z., Keddie, J., Adam, L., Pineda, O., Ratcliffe, O.J., Samaha, R.R., et al. (2000). *Arabidopsis* transcription factors: genome-wide comparative analysis among eukaryotes. *Science* 290, 2105–2110.
- Schellenberger Costa, B., Sachse, M., Jungandreas, A., Bártulos, C.R., Gruber, A., Jakob, T., Kroth, P.G., and Wilhelm, C. (2013). Aureochrome 1a is involved in the photoacclimation of the diatom *Phaeodactylum tricornutum*. *PLoS One* 8, e74451.
- Serif, M., Lepetit, B., Weißert, K., Kroth, P.G., and Rio Bártulos, C. (2017). A fast and reliable strategy to generate TALEN-mediated gene knockouts in the diatom *Phaeodactylum tricornutum*. *Algal Res.* 23, 186–195.
- Sims, P.A., Mann, D.G., and Medlin, L.K. (2006). Evolution of the diatoms: insights from fossil, biological and molecular data. *Phycologia* 45, 361–402.

Smith, S.R., Dupont, C.L., McCarthy, J.K., Broddrick, J.T., Obornik, M., Horák, A., Füssy, Z., Cihlář, J., Kleessen, S., Zheng, H., et al. (2019). Evolution and regulation of nitrogen flux through compartmentalized metabolic networks in a marine diatom. *Nat. Commun.* *10*, 4552.

Suetsugu, N., and Wada, M. (2013). Evolution of three LOV blue light receptor families in green plants and photosynthetic stramenopiles: phototropin, ZTL/FKF1/LKP2 and aureochrome. *Plant Cell Physiol.* *54*, 8–23.

Takahashi, F., Yamagata, D., Ishikawa, M., Fukamatsu, Y., Ogura, Y., Kasahara, M., Kiyosue, T., Kiyama, M., Wada, M., and Kataoka, H.

(2007). AUREOCHROME, a photoreceptor required for photomorphogenesis in stramenopiles. *Proc. Natl. Acad. Sci. U S A* *104*, 19625–19630.

Tanaka, A., De Martino, A., Amato, A., Montsant, A., Mathieu, B., Rostaing, P., Tirichine, L., and Bowler, C. (2015). Ultrastructure and membrane traffic during cell division in the marine pennate diatom *Phaeodactylum tricorutum*. *Protist* *166*, 506–521.

Valle, K.C., Nymark, M., Aamot, I., Hancke, K., Winge, P., Andresen, K., Johnsen, G., Brembu, T., and Bones, A.M. (2014). System responses to equal doses of photosynthetically usable

radiation of blue, green, and red light in the marine diatom *Phaeodactylum tricorutum*. *PLoS One* *9*, e114211.

Veluchamy, A., Lin, X., Maumus, F., Rivarola, M., Bhavsar, J., Creasy, T., Ó'Brien, K., Sengamalay, N.A., Tallon, L.J., Smith, A.D., et al. (2013). Insights into the role of DNA methylation in diatoms by genome-wide profiling in *Phaeodactylum tricorutum*. *Nat. Commun.* *4*, 2091.

Wilhelm, C., Jungandreas, A., Jakob, T., and Goss, R. (2014). Light acclimation in diatoms: from phenomenology to mechanisms. *Mar. Genomics* *16*, 5–15.

iScience, Volume 23

Supplemental Information

The Aureochrome Photoreceptor

PtAUREO1a Is a Highly Effective

Blue Light Switch in Diatoms

Marcus Mann, Manuel Serif, Thomas Wrobel, Marion Eisenhut, Shvaita Madhuri, Samantha Flachbart, Andreas P.M. Weber, Bernard Lepetit, Christian Wilhelm, and Peter G. Kroth

Figure S1: Volcano scatter plots displaying the probability (FDR adjusted p-value) against the log₂-fold change. Related to Fig. 2.

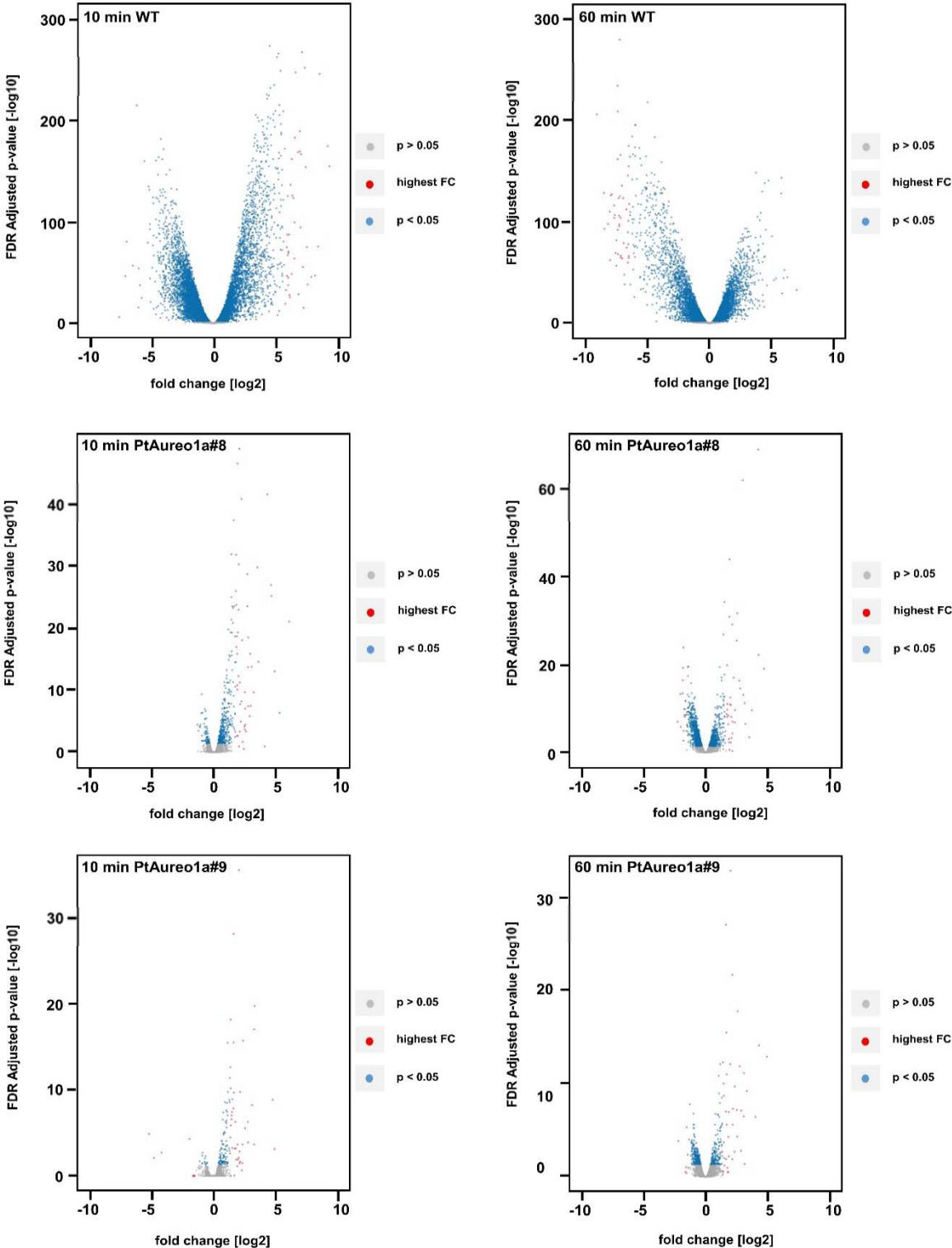


Figure S1: Volcano scatter plots displaying the probability (FDR adjusted p-value) against the log₂-fold change. In wild type cells, a large number of genes are either up- or down-regulated after a shift to 10 min of blue light, while after 60 min the majority of genes is down-regulated. Knockout mutants *PtAureo1a#8* und *#9* show a similar pattern, but much weaker, as much less genes are regulated.

Figure S2: Clustering of up- and downregulated genes of groups of transcription factors from WT cells. Related to Fig. 5.

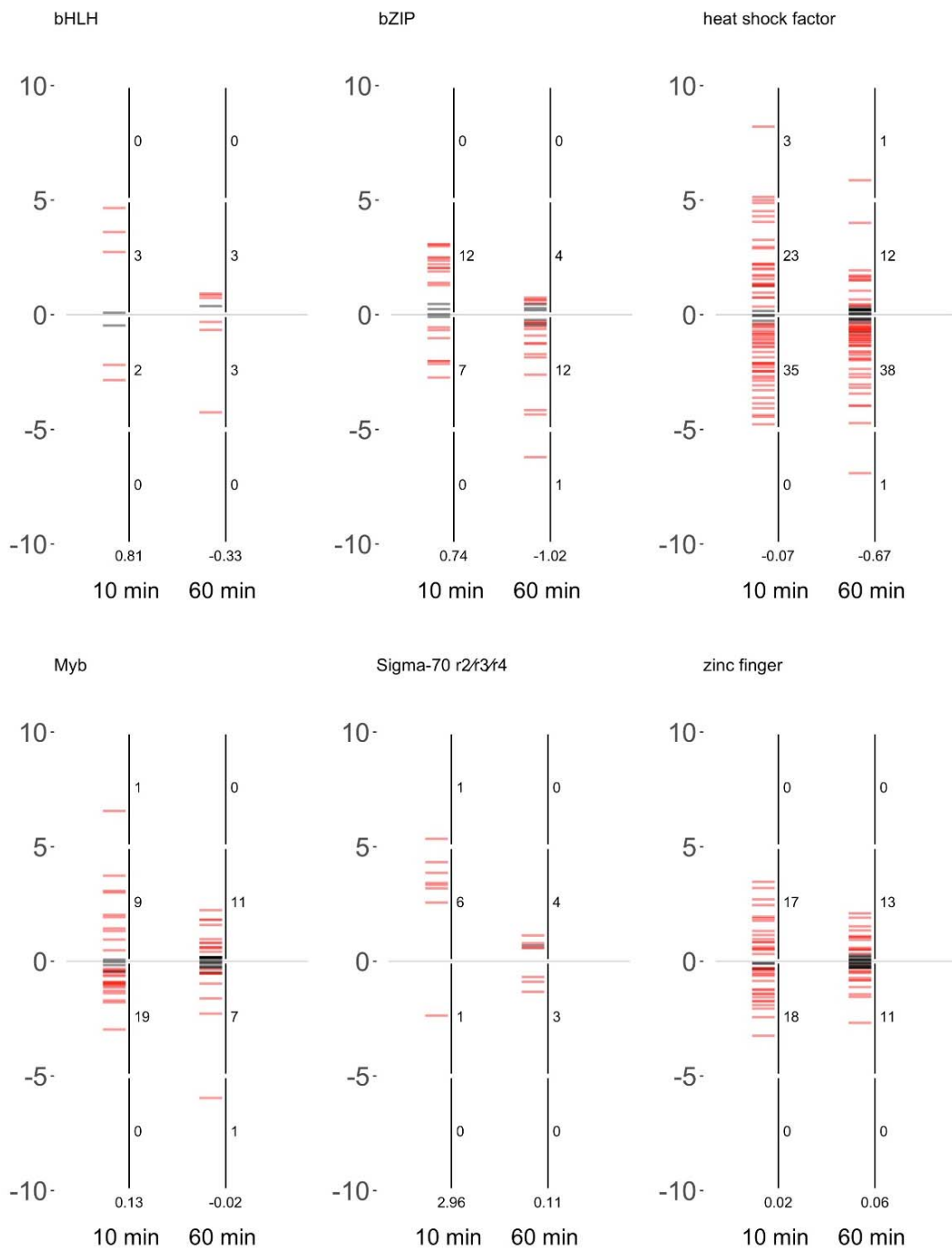


Figure S2: Clustering of up- and downregulated genes of groups of transcription factors from WT cells. The y-axis refers to log₂-fold change at the respective time point compared to time point 0, the small numbers at the right side of the vertical axis indicate the number of genes regulated in the respective log₂-fold interval covering five units and the small number below the y-axis refers to the average log₂-fold change of the whole transcription factor family. Red bars: significantly changes (P < 0.05); black bars: not significantly changes (P > 0.5). Most of the transcription factor families (with the exception of zinc finger proteins and heat shock factors) show more genes to be upregulated than downregulated after 10 min. After 60 min, most families show a balanced distribution or slight increase of downregulated genes (with the exception of zinc finger proteins).

Figure S3: Changes in expression of selected genes. Related to Transparent Methods.

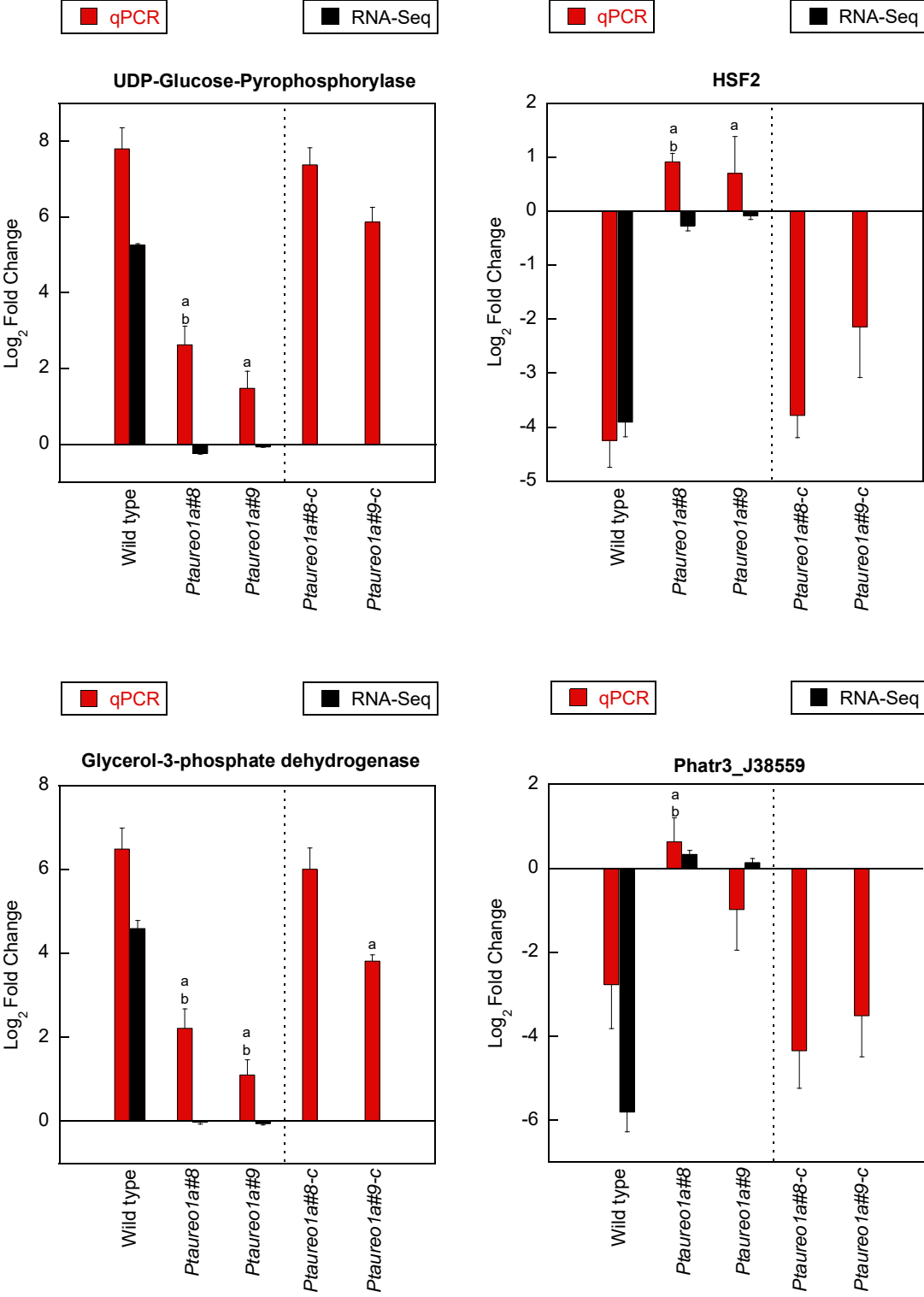


Figure S3: Changes in expression of selected genes (UDP glucose pyrophosphorylase (Phatr3_EG02613), HSF2 (Phatr3_J55070), glycerol-3-phosphate dehydrogenase (Phatr_36821) and the undescribed gene Phatr3_J38559) after a shift from red light (28 $\mu\text{mol photons m}^{-2} \text{s}^{-1}$, measured with a LICOR planar quantum sensor) to 10 minutes of blue light (18 $\mu\text{mol photons m}^{-2} \text{s}^{-1}$), indicated in \log_2 -fold changes, in batch cultures of *P. tricornutum* WT, *Ptaureo1a#8*, *Ptaureo1a#9* and one complemented line for each knockout (*Ptaureo1a#8-c*, *Ptaureo1a#9-c*), determined by qPCR analyses of three biological replicates each. On the left side, genes that are upregulated upon a 10 min BL shift in the WT, based on the RNA-Seq analyses, are indicated. On the right side, genes that are downregulated upon a 10 min BL shift in WT cells, based on the RNA-Seq analyses, are indicated. For comparison, the \log_2 -fold changes for the respective genes, calculated from the TPM values of the RNA-Seq dataset, are indicated in black columns. Note that complemented lines have only been analyzed by qPCR and therefore are separated from WT and knockout lines by the dotted vertical line. Statistical significance for qPCR samples was determined using the Pairwise Fixed Reallocation Randomization Test performed by REST with 2000 randomizations. 'a' indicates statistical significance with $p < 0.05$ compared to the WT, while 'b' indicates statistical significance of the knockout line compared to the respective complemented line with $p < 0.05$. Standard error is indicated. A list of primers used is shown in Supplementary Table 1.

Figure S4: Log₂-fold transcript changes of putative histone modifying genes. Related to Fig. 6.

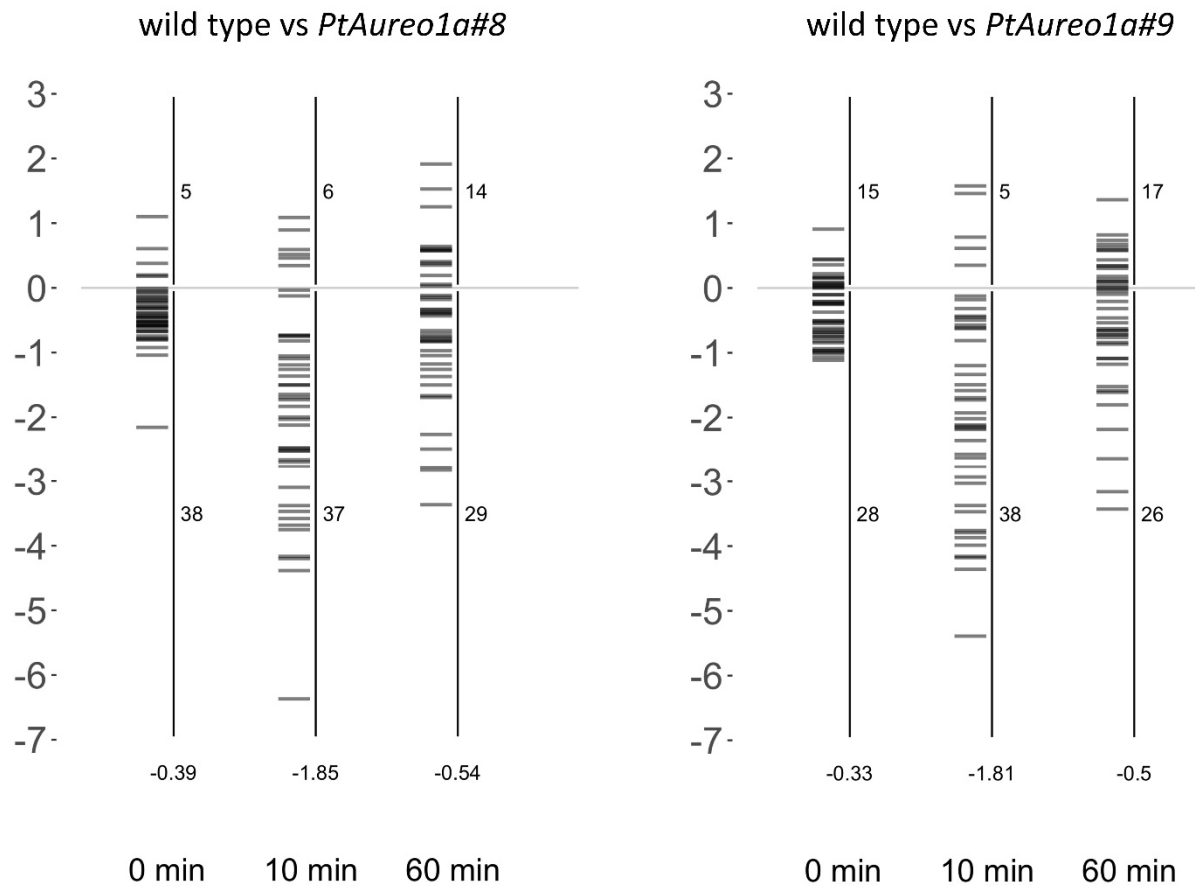


Figure S4: Log₂-fold transcript changes of putative histone modifying genes in WT vs *PtAureo1a#8* (a) and WT vs *PtAureo1a#9* (b) at time point 0, 10 and 60 min. The mean log₂-fold change for each gene is indicated as an individual bar. The numbers on the right side of the vertical axes indicate the amount of higher and lower expressed genes in the WT, respectively. The numbers below each plot indicate the average log₂-fold transcript change of all histone-modifying genes at the respective time point. The following genes have been included in the analyses (for details, see master tables: Supplemental Table 3/4 in individual files):

Phatr3_EG00952.t1, Phatr3_EG01307.t1, Phatr3_EG01943.t1, Phatr3_EG02126.t1, Phatr3_EG02442.t1, Phatr3_J1785.t1, Phatr3_J2957.t1, Phatr3_J3062.t1, Phatr3_J4423.t1, Phatr3_J4821.t1, Phatr3_J8891.t1, Phatr3_J9278.t1, Phatr3_J11358.t1, Phatr3_J35869.t1, Phatr3_J41559.t1, Phatr3_J42892.t1, Phatr3_J42944.t1, Phatr3_J43274.t1, Phatr3_J43627.t1, Phatr3_J43708.t1, Phatr3_J43919.t1, Phatr3_J44745.t1, Phatr3_J44757.t1, Phatr3_J44807.t1, Phatr3_J45431.t1, Phatr3_J45548.t1, Phatr3_J45703.t1, Phatr3_J45764.t1, Phatr3_J45906.t1, Phatr3_J46372.t1, Phatr3_J47425.t1, Phatr3_J49800.t1, Phatr3_J50465.t1, Phatr3_J50482.t1, Phatr3_J50848.t1, Phatr3_J51026.t1, Phatr3_J51040.t1, Phatr3_J51345.t1, Phatr3_J51406.t1, Phatr3_J54343.t1, Phatr3_J54505.t1, Phatr3_Jdraft1647.t1, Phatr3_Jdraft292.t1

Supplemental Table S1: Primers used for qPCR analyses. Related to Figure S3. The gene names refer to the Phaeodactylum genome database Phatr3 (https://protists.ensembl.org/Phaeodactylum_tricornutum/Info/Index)

Name	Forward primer sequence	Reverse primer sequence
UDP-Glucose-Pyrophosphorylase (Phatr3_EG02613) - fw	5'-GTCTCGTCTCGGGTGATTCC-3'	
UDP-Glucose-Pyrophosphorylase - rev		5'-CGTCCCCCTTGACTGGCAA-3'
Glycerol-3-phosphate dehydrogenase (Phatr_36821) - fw	5'-TCATCGGTAGCGGTAAGTGG-3'	
Glycerol-3-phosphate dehydrogenase - rev		5'-ACCTGCGATTGAAAAAGGG-3'
HSF2 (Phatr3_J55070) - fw	5'-ATGACTTACGCATCTCCCAATA-3'	
HSF2 - rev		5'-GGGTCGGTCAGTAGTTTTTCGAG-3'
Phatr3_J38559 - fw	5'-TACTTGGAACGTCTCGGTTCG-3'	
Phatr3_J38559 - rev		5'-TAGAAAGCGGTTGCCAAGAC-3'
Phatr3_J47943 - fw	5'-ATGCCGACACAGTCTACCG-3'	
Phatr3_J47943 - rev		5'-GGAGAGGTGGTTGTTGTTGC-3'

Transparent methods

Cultivation and harvesting of cells for RNA-Seq and qPCR

WT and PtAureo1a knockout strains K8 and K9 were cultured semi-continuously, in order to prevent nutrient limitation, as described in (Schellenberger Costa et al., 2013). The light intensity of blue and red light was adjusted to yield the same amount of photosynthetically absorbed radiation (Q_{phar} 10 $\mu\text{mol photons m}^{-2} \text{s}^{-1}$) according to (Gilbert et al., 2000). Cells were adapted to a 14h/10h day night cycle with red light (28 $\mu\text{mol photons m}^{-2} \text{s}^{-1}$, 659 \pm 11 nm) at 20°C for 10 days and then were shifted to blue light (18 $\mu\text{mol photons m}^{-2} \text{s}^{-1}$, 469 \pm 10 nm). Samples were taken at time point $t=0$ (red light) as well as 10 min and 60 min of blue light: 50 ml of cells were filtered onto 1.2 μm RTTP polycarbonate filters (Merck-Millipore, Darmstadt, Germany), flash-frozen in liquid nitrogen and stored at -80°C until further use in RNA-Seq experiments. For verification of the transcriptome data, the expression of some selected genes in the WT line, the two PtAureo1a KO strains K8 and K9, and the two Aureo1a complemented lines Aureo1a8 Co56 (= *Ptaureo1a#8-c*) and Aureo1a9 Co59 (= *Ptaureo1a#9-c*) were analyzed via qPCR. The latter two strains are described and characterized in (Madhuri et al., 2019). The strains were cultivated in Erlenmeyer flasks on an orbital shaker in an Algaetron incubation chamber (PSI, Czech Republic) for 10 days at 20°C and 28 $\mu\text{mol photons m}^{-2} \text{s}^{-1}$ of red light (636 nm) and then shifted to blue light (18 $\mu\text{mol photons m}^{-2} \text{s}^{-1}$, 440 nm) for 10 min.

Sample preparation for RNA-Seq

RNA was extracted from the filtered cells using the PeqGOLD RNApure and PeqGOLD RNA extraction kits (VWR, Darmstadt, Germany). Potential contamination with residual DNA was removed by an on-column digest with the PeqGOLD DNase I digest kit (VWR). Extracted RNA was quality-controlled with a spectrophotometer, by separation on an agarose gel, as well as on a 2100 bioanalyzer (Agilent, Waldbronn, Germany). cDNA libraries were prepared from 1 μg RNA using the TruSeq™ RNA Sample Prep Kit v2 (Illumina Inc., San Diego, USA). cDNA library generation and sequencing were performed with the Illumina HiSeq2000 in the paired end mode.

Bioinformatical analyses of the sequencing data and statistical information

Transcript abundances were determined by mapping the reads against the *P. tricornutum* CCAP 1055/1 genome (Release 27, downloaded June 14, 2015) in Ensembl

(http://protists.ensembl.org/Phaeodactylum_tricornutum/Info/Index, cDNA) using the CLC genomics workbench (<https://www.qiagenbioinformatics.com/>) with default parameters. Downstream analysis was performed in R version 3.6.1 (www.r-project.org). Differential gene expression was determined using edgeR (Robinson et al., 2009) on raw counts in GLM Fit mode with subsequent common and tagwise dispersion estimation. Principal component analyses and k-means clustering was performed on Z-scores calculated from TPM values. Samples were called significantly different if adjusted P value was <0.05. Gene enrichment for the k-means clusters was determined via the Fishers exact test using hand curated Mapman categories. To this end, the coding sequences from the *P. tricornutum* genome were compared to their *Arabidopsis* counterpart via bidirectional BLAST and the corresponding Mapman categories used as a starting point. BLAST results as well as the final Mapman categories are provided in Supplementary Tables 3 and 4. All P-values were Benjamini-Hochberg corrected before further analysis (Benjamini and Hochberg, 1995). The complete RNA-Seq data is also provided in Supplementary Tables 3 and 4. The read data are deposited at the National Center for Biotechnology Information Gene Expression Omnibus under accession number GSE158698. PCA analyses in Fig. 1 and the hierarchical cluster analyses were performed using the CLC genomics workbench software. For Figs. 3-5, TPM values of selected genes were plotted and statistically analyzed using GraphPad Prism version 8.4.2 (San Diego, CA). Two-way ANOVA with comparing every mean with every other mean was performed including Tukey test to correct for multiple comparisons.

Quantitative Real Time PCR (q-PCR)

RNA isolation for qPCR analysis was performed as described above. cDNA was synthesized using the Primescript kit (Takara Bio Europe, France). qPCR was performed with a 7500 Fast RT-PCR system (Applied Biosystems, USA) using a 2-step protocol. Each strain was measured in biological triplicates, and, on top, each gene per sample was measured in technical triplicates. Cycle threshold values and gene amplification efficiencies were obtained by utilizing PCR Miner 4.0 (Zhao and Fernald, 2005). Relative transcript levels were calculated according to (Pfaffl, 2001; Pfaffl et al., 2002). As 18S was not stably expressed under RL to BL shift conditions, we tested four genes which were stable during the shift and used one of them i.e. Phatr3_J47943.t1 (accession no. NC_011683) as reference gene. Primer sequences for all tested genes are supplied in Supplementary Table 1. Significance was tested using the Pairwise Fixed Reallocation Randomization Test performed by REST 2006 with 2000 randomizations (Pfaffl et al., 2002).

References for Supplemental Information

- Benjamini, Y., and Hochberg, Y. (1995). Controlling the False Discovery Rate: A Practical and Powerful Approach to Multiple Testing. *Journal of the Royal Statistical Society: Series B (Methodological)* 57, 289-300.
- Gilbert, M., Domin, A., Becker, A., and Wilhelm, C. (2000). Estimation of Primary Productivity by Chlorophyll a in vivo Fluorescence in Freshwater Phytoplankton. *Photosynthetica* 38, 111-126.
- Madhuri, S., Río Bártulos, C., Serif, M., Lepetit, B., and Kroth, P.G. (2019). A strategy to complement PtAUREO1a in TALEN knockout strains of *Phaeodactylum tricornutum*. *Algal Research* 39, 101469.
- Matthijs, M., Fabris, M., Obata, T., Foubert, I., Franco-Zorrilla, J.M., Solano, R., Fernie, A.R., Vyverman, W., and Goossens, A. (2017). The transcription factor bZIP14 regulates the TCA cycle in the diatom *Phaeodactylum tricornutum*. *The EMBO Journal* 36, 1559-1576.
- Pfaffl, M.W. (2001). A new mathematical model for relative quantification in real-time RT-PCR. *Nucleic Acids Research* 29, e45.
- Pfaffl, M.W., Horgan, G.W., and Dempfle, L. (2002). Relative expression software tool (REST©) for group-wise comparison and statistical analysis of relative expression results in real-time PCR. *Nucleic Acids Research* 30, e36-e36.
- Rayko, E., Maumus, F., Maheswari, U., Jabbari, K., and Bowler, C. (2010). Transcription factor families inferred from genome sequences of photosynthetic stramenopiles. *New Phytol* 188, 52-66.
- Robinson, M.D., McCarthy, D.J., and Smyth, G.K. (2009). edgeR: a Bioconductor package for differential expression analysis of digital gene expression data. *Bioinformatics* 26, 139-140.
- Schellenberger Costa, B., Sachse, M., Jungandreas, A., Bartulos, C.R., Gruber, A., Jakob, T., Kroth, P.G., and Wilhelm, C. (2013). Aureochrome 1a is involved in the photoacclimation of the diatom *Phaeodactylum tricornutum*. *PLOS ONE* 8, e74451.
- Zhao, S., and Fernald, R.D. (2005). Comprehensive Algorithm for Quantitative Real-Time Polymerase Chain Reaction. *Journal of Computational Biology* 12, 1047-1064.